TRANSPORT EQUATION OF THE MEAN ENERGY DISSIPATION RATE ON THE AXIS OF A TURBULENT ROUND JET

Nathan Lefeuvre
School of Engineering
University of Newcastle
Australia
nathan.lefeuvre@uon.edu.au

Lyazid Djenidi
School of Engineering
University of Newcastle
Australia
lyazid.djenidi@newcastle.edu.au

Robert Antonia
School of Engineering
University of Newcastle
Australia
robert.antonia@newcastle.edu.au

ABSTRACT

The transport equation of the mean turbulent energy dissipation ($\overline{\varepsilon}$) along the axis of a turbulent round jet is examined in the context of the scale-by-scale energy budget. The previously well established $(x-x_o)^{-4}$, where x_o is the virtual origin, dependence of $\overline{\varepsilon}$ along the jet axis is shown to be consistent with the limits at both small and large-scale of this budget. It is found that the isotropic form of the transport equation for $\overline{\varepsilon}$ requires the sum S_u+2G_u/R_λ to be constant along the jet axis for given initial conditions, where S_u is the skewness, G_u is the destruction coefficient and R_λ is the Taylor micro scale Reynolds number. These results are consistent the theoretical analysis of Thiesset *et al.* (2014) who showed that $S_u+2G_u/R_\lambda \sim R_\lambda^{-1}$. The way that the sum S_u+2G_u/R_λ approaches zero at high R_λ, as required for stationary isotropic turbulence, is discussed.

INTRODUCTION

The streamwise evolution of $\overline{\varepsilon}$ along the axis of a turbulent round jet was investigated by Friehe *et al.* (1971) and Antonia *et al.* (1980). It is generally accepted that in turbulent flows and when R_λ is large, $\overline{\varepsilon}$ follows the relation

$$\overline{\varepsilon} = C_\varepsilon \frac{u'^3}{L_u}, \tag{1}$$

where L_u and u' are the integral length scale and the *rms* of the longitudinal velocity fluctuation, respectively, and C_ε is an empirical constant. In decaying turbulent flows, such as grid-generated turbulence, a plane wake and a round jet, L_u and u' are function of the distance $(x-x_o)$ (x_o is the virtual origin). On the axis of a round jet, the streamwise variations of L_u and u' vary with $(x-x_o)$ and $(x-x_o)^{-1}$, respectively, while $L_u \sim (x-x_o)^{1/2}$ and $u' \sim (x-x_o)^{-1/2}$ on the centreline of a self-preserving plane wake. Consequently, the streamwise evolution of $\overline{\varepsilon}$ is proportional to $(x-x_o)^{-4}$ for a round jet and $(x-x_o)^{-2}$ for a plane wake. Mi *et al.* (2013) established that the prefactor for $\overline{\varepsilon} \sim (x-x_o)^{-4}$ ceases to depend on the Reynolds number Re_D ($\equiv U_j D/\nu$, where U_j is the jet exit velocity and D is the nozzle diameter) when Re_D exceeds 10^4. Note however that the condition $C_\varepsilon = const$ is not essential for deriving the power-law dependence $(x-x_o)^{-4}$ of $\overline{\varepsilon}$. Self-preservation is sufficient for this purpose.

Self-preservation (hereafter denoted SP) rests on the assumption that the flow is governed by a set of length and velocity scales. Townsend (1956) carried out a systematic SP analysis on the mean momentum and mean turbulent kinetic energy equations for various turbulent flows (wake, jet and wall flows). More relevant to the present work, SP has been used to describe the streamwise evolution of one-point turbulent statistics in a turbulent round jet (George (1989); George & Gibson (1992); Panchapakesan & Lumley (1993)). Using a SP analysis, George (1989) showed that, for a given turbulent round jet, the streamwise variation of the length and velocity scales are not universal and may depend on the initial conditions. His SP analysis is supported by experimental evidence (*e.g.* George (1989); George & Gibson (1992); Wygnanski *et al.* (1986)). Extending the SP analysis to two-point statistics is expected to provide a further assessment of the evolution of the turbulence at a given scale. Ewing *et al.* (2007) carried out a SP analysis on the governing equations for the two-point velocity correlation in a turbulent round jet. However, their analysis cannot predict the power-law $\overline{\varepsilon} \sim (x-x_o)^{-4}$ along the axis of the jet. On the other hand, Thiesset *et al.* (2014) who carried out a SP analysis on the transport equation of $\overline{(\delta u)^2}$ ($\overline{(\delta u)} = u(x+r)-u(x)$ is the velocity increment in the longitudinal direction, and r is the separation between 2 points) on the axis of the jet not only showed that $\overline{\varepsilon}$ follows the law $A_\varepsilon(x-x_o)^{-4}$ but they were also able to derive a theoretical expression for the prefactor A_ε.

The transport equation of $\overline{(\delta u)^2}$ on the jet centreline, which can be seen as the energy budget at each spatial separation r from the smallest to the largest scale, is given by:

$$-\overline{(\delta u)^3}+6\nu\frac{\partial\overline{(\delta u^2}}{\partial r}-\frac{3}{r^4}\int_0^r s^4\overline{U}\frac{\partial\overline{(\delta u)^2}}{\partial x}ds \\ -\frac{3}{r^4}\int_0^r s^4 2\left(\overline{(\delta u)^2}-\overline{(\delta v)^2}\right)\frac{\partial\overline{U}}{\partial x}ds=\frac{4}{5}\overline{\varepsilon}r. \quad (2)$$

Burattini *et al.* (2005*b*,*a*) provided adequate experimental support for (Eq. 2). At the large separations, Eq. (2) yields the one-point budget of $\overline{q^2}$

$$-\frac{1}{2}\overline{U}\frac{\partial\overline{q^2}}{\partial x}-\left(\overline{u^2}-\overline{v^2}\right)\frac{\partial\overline{U}}{\partial x}=\overline{\varepsilon}, \quad (3)$$

where $\overline{q^2}=\overline{u^2}+2\overline{v^2}$ by virtue of axisymmetry. This equation shows that $\overline{\varepsilon}$ represents the balance between the advection and production (1st and second terms, respectively, on the left side). Note that the pressure-transport term in Eq. (3) is neglected as was done by Panchapakesan & Lumley (1993), Burattini *et al.* (2005*a*) and Taub *et al.* (2013).

The application of a SP analysis to Eq. (2), shows that the round jet can satisfy simultaneously solutions at all scales provided any characteristic Reynolds number is constant. This implies that the Reynolds number based on any characteristic length scale (*e.g.* λ, η, L or δ, the Taylor-micro scale, Kolmogorov length scale, the integral length,or half-width of the jet) and velocity scale (*e.g.* u' or v_K, the Kolmogorov velocity scale) is constant. Therefore, a round jet satisfying SP admits a SP solution that is independent of the SP variables used. Thiesset *et al.* (2014) extended the analysis of Burattini *et al.* (2005*a*) and examined consequences of self-preservation for Eq. (2) on the axis of a round jet. By assuming local isotropy and a power law decay they showed that Eq. (2) can be reduced to

$$S_u+2G_u/R_\lambda=\frac{90}{7(2+R)R_\lambda} \quad (4)$$

in the limit of $r\to 0$, with

$$S_u=\frac{\overline{(\partial u/\partial x)^3}}{\overline{(\partial u/\partial x)^2}^{3/2}} \quad (5)$$

$$G_u=\overline{u^2}\frac{\overline{(\partial u/\partial x)^2}}{\overline{(\partial u/\partial x)^2}^2} \quad (6)$$

and $R=\overline{v^2}/\overline{u^2}$. S_u is the velocity derivative skewness and G_u is the destruction coefficient, sometimes referred to as the palinstrophy coefficient; they represent the production and dissipation of $\overline{\varepsilon}$, respectively. The relation (4) highlights the dependence between large and small scales through the large scale anisotropy ratio R for finite Reynolds numbers. As $R_\lambda\to 0$, $S_u+2G_u/R_\lambda\to\infty$, indicating that large and small scales becomes uncorrelated as the Reynolds number becomes very large; it further indicates that the small-scale motions approach stationary as $R_\lambda\to\infty$. Interestingly, Thiesset *et al.* (2014) compared Eq. 4 with its counter part in grid turbulence and found that the small scales approach to stationarity differently between in two flows.

The present study aims at complementing and extending the work of Thiesset *et al.* (2014). We experimentally investigate the consequence of SP on the transport equation of $\overline{\varepsilon}$. In particular, terms of Eq. (4) are measured and their streamwise evolution assessed along the centreline of the turbulent round jet at several Reynolds numbers ranging from 10^4 to 10^5. We will also briefly discuss the behaviour of eq. (4) as R_λ increases.

EXPERIMENTAL SETUP

The turbulent jet is generated by an open circuit wind tunnel. A contraction is attached to the tunnel exit with an area contraction of 85 : 1. The jet exits through a nozzle having a diameter $D=55mm$. A circular plate of diameter 100mm was mounted at the nozzle exit and flush with the nozzle exit section to improve the jet flow at the exit, which had a top-hat velocity profile; the incoming boundary layer at the nozzle lip is laminar, although not quite Blasius. The Reynolds numbers Re_D, based on the exit velocity, U_j, and D, was varied from about 10000 to 100000. The velocity is measured with a single hot-wire etched from $PT-10\%Rh$ to a diameter of $d_w=1.2\mu m$ and the active length l_w was chosen so as to have an aspect ratio l_w/d_w of nearly 200. Further details of the experimental setup can be found in Burattini *et al.* (2005*a*).

Hot wire velocity measurements in turbulent flows may lead to various problems if care is not taken. One such problem relates to the use Taylor's hypothesis, to convert temporal statistics to spatial statistics. This hypothesis is acceptable when the relative turbulence intensity, u_1'/U, is small. In this case, the convection velocity is assumed to be constant and equal to the mean velocity. In the far field of an axisymmetric jet, the turbulence intensity is about 25% (Mi *et al.* (2013)) which can lead to non negligible errors to statistical results. To remedy this problem, in the present work, we applied a correction to the instantaneous velocity signal. A modified version of Taylor's hypothesis (MTH) has been used based the method implemented by Kahalerras *et al.* (1998). The effect of the spatial correction is significant on the statistics of the velocity fluctuations, such as the $1D$ energy spectrum of u as shown Figure (1). This shows that the major effects of MTH are concentrated at the high wave numbers of the spectrum, *i.e.* at the small scales. MTH helps to minimise the "artificial energy" added at the high wave numbers by the use of Taylor's hypothesis, as observed in Figure (1). In the context of this work, the application of the MTH is essential for calculating accurately turbulent quantities, such as $\overline{\varepsilon}$, R_λ, S_u or G_u, quantities that are the focus of this study.

RESULTS

Thiesset *et al.* (2014) showed that carrying out a SP analysis on Eq. (2) on the centreline of the turbulent round jet leads to the following SP solution for $\overline{\varepsilon}$:

$$\frac{\overline{\varepsilon}D}{U_J^3}=A_\varepsilon\left(\frac{x-x_o}{D}\right)^{-4} \quad (7)$$

where A_ε is constant. Further, Thiesset *et al.* (2014) pro-

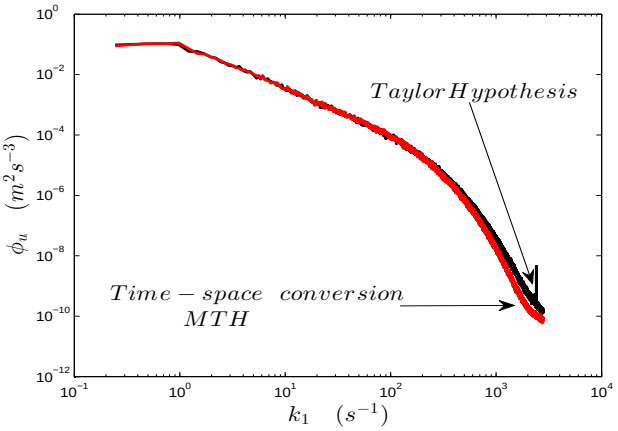


Figure 1. The effect of Taylor's hypothesis on the velocity spectrum on the axis of the axisymmetric jet for $Re_D = 8.9 \times 10^4$.

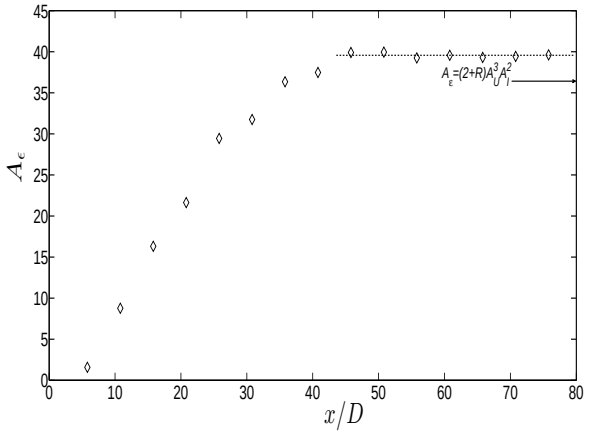


Figure 2. Axial variation of A_ε versus x/D for $Re_D = 1 \times 10^5$. The value of A_ε inferred from the expression (8) is marked by an arrow.

posed an expression for A_ε of the form

$$A_\varepsilon = (2+R)A_U^3 A_I^2 \tag{8}$$

where A_U is the prefactor of the power-law $(U/U_J = Au((x-x_o)/D)^{-1}$ for the mean velocity, U, and $A_I = (\sqrt{\overline{u^2}}/U)$.

Figure (2), which shows the centreline variation of A_ε, indicates that A_ε becomes constant for $x/D \geq 45$, marking thus the start of SP solutions on the jet axis. The values shown in figure (2) are obtained by plotting $\frac{\overline{\varepsilon}D}{U_j^3}\left(\frac{x-x_o}{D}\right)^4$, where x_0 was found to be about $4.5D$; x_o was obtain from the distributions of $\overline{u^2}/U^2$. The values of A_ε shown in Figure (2) and lying on the plateau are about 9% larger than the value inferred from the relation (8), where $R = 2/3$ and A_U and A_I, estimated from the measurements, are about 6 and 0.25, respectively. Interestingly, the value of A_ε proposed by Friehe *et al.* (1971) and commonly used is 48, *i.e.* about 33% larger than the present predicted value. Thiesset *et al.* (2014) argued that any differences between the predicted and measured values of A_ε are mainly associated with an error in x_o. Indeed, a variation in x_o may impart a non negligible variation in $(x-x_o)^4$ and thus affect the value

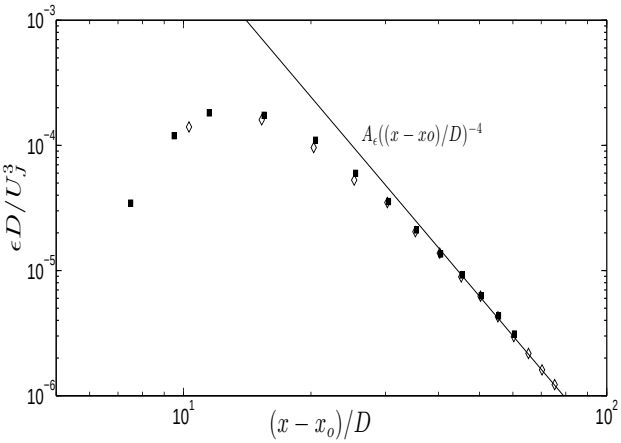


Figure 3. Axial variation of $\overline{\varepsilon}$ versus x/D. ■: $Re_D = 8.9 \times 10^4$, ◊: $Re_D = 1 \times 10^5$. The line is calculated with expression (8) where $A_\varepsilon = 39$ and $x_o/D = -4.5$

of A_ε when it is estimated experimentally from the plot $\frac{\overline{\varepsilon}D}{U_j^3}\left(\frac{x-x_o}{D}\right)^4$. Nonetheless, the present relatively good agreement between the predicted and measured values of A_ε indicates that not only the value of x_o seems correct but the neglect the viscous diffusion and pressure transport terms in Eq. (2) seems justifiable.

Examples of the centreline variations of $\frac{\overline{\varepsilon}D}{U_j^3}$ are reported in Figure (3) for $Re_D = 8 \times 10^4$ and 1×10^5. The isotropic form $\overline{\varepsilon}_{iso} = 15\nu\overline{(\partial u/\partial x)^2}$ was used to estimate $\overline{\varepsilon}$. Since we are investigating the isotropic form for Eq. (2) in the limit of $r \to 0$, we use $\overline{\varepsilon}_{iso}$ as the surrogate of $\overline{\varepsilon}$ in the rest of the paper. It should be noted that some justification for identifying $\overline{\varepsilon}$ with $\overline{\varepsilon_{iso}}$ is provided by earlier measurements of all the temperature dissipation rate which seemed to satisfy isotropy reasonably well on the axis of the jet (Antonia & Mi (1993) and Darisse *et al.* (2014)). The SP analysis of Thiesset *et al.* (2014) on Eq. (2) shows that $\overline{\varepsilon}$ should vary as x^{-4} on the centreline of the jet. This is well confirmed in the far field of the jet as illustrated in Figure (3), which shows $\frac{\overline{\varepsilon}D}{U_j^3}$ versus $(x-x_o)/D$. The predicted values of $\frac{\overline{\varepsilon}D}{U_j^3}$ calculated from expression (8) with $A_\varepsilon = 39$ and $x_0 = -4.5D$ are also reported in the figure (see the solid line) and match very well the data for $(x-x_o)/D \geq 40$.

The SP behaviour of $\overline{\varepsilon}$ shown in Figure (3) should, in conformity with the SP analysis as applied to Eq. (2), require the constancy of R_λ. This is indeed observed in Figure (4), which shows the centreline evolution of R_λ for several values of the jet Reynolds number Re_D. The data of Mi *et al.* (2013) and Burattini *et al.* (2005*a*) are also reported in the figure. Note that for $Re_D = 1 \times 10^4$, R_λ does not appear to be constant suggesting that SP is not satisfied at this Reynolds number. When $Re_D \geq 2 \times 10^4$, R_λ exhibits a clear plateau over a significant range of x/D. Note though that the beginning of the plateau (*i.e.* start of SP solutions) moves downstream as Re_D increases. For example, SP starts at $x/D \simeq 15$ and 40 when $Re_D = 3.4 \times 10^4$ and 13×10^4, respectively. The figure clearly reveals that the higher Re_D is, the larger x/D should be before SP is reached (or can be observed). For example, when $Re_D \geq 1 \times 10^5$, one is required to carry out measurements beyond x/D at least equal to 30 to start to observe the jet evolving in SP manner.

The centreline evolution of both $\overline{\varepsilon}$ and R_λ confirms that

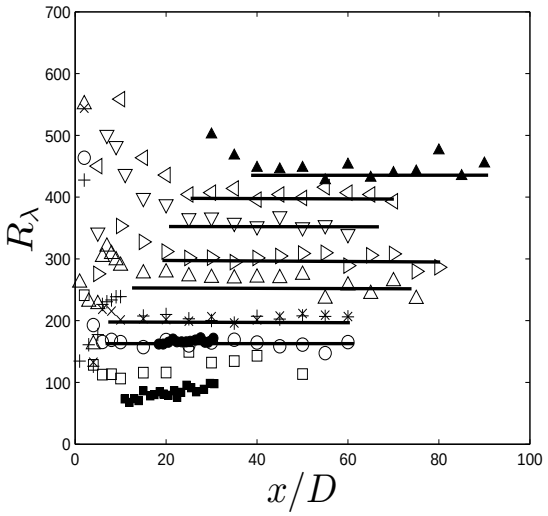


Figure 4. Axial variation of R_λ versus x/D. Present data from bottom to top: $Re_D = 1\times10^4$, 2×10^4, 3.4×10^4, 5.3×10^4, 7×10^4, 8.9×10^4 and 10×10^4. The horizontal lines are the average values along x, calculated from the streamwise location when R_λ reaches a constant. Mi *et al.* (2013): ■, $Re_D = 1\times10^4$; •, $Re_D = 2\times10^4$. Burattini *et al.* (2005*a*): ▲, $Re_D = 13\times10^4$.

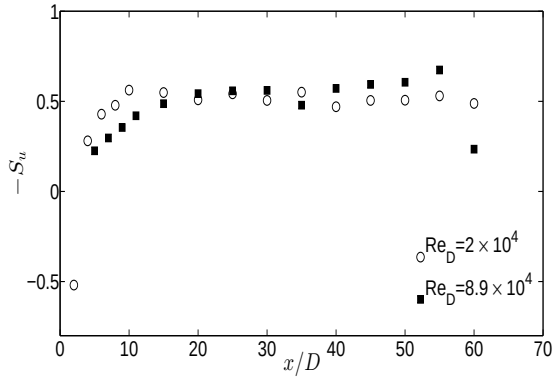


Figure 5. Centreline variation of S_u. ◯: $Re_D = 2\times10^4$, ■: $Re_D = 8.9\times10^4$.

SP is well satisfied in the present turbulent round jet. Note that since R_λ is constant during the decay then the left term of Eq. (4) must also be constant (under the condition that R remains constant). This indicates that the balance between the production and destruction of $\overline{\varepsilon}$, S_u and G_u, respectively, remains constant during the decay. In that context, it is of interest to assess the individual behaviours of both S_u and G_u.

Figures 5 and (6) show the centreline variations of S_u and G_u/R_{lambda} for $Re_D = 2\times10^4$ and 8.9×10^4. Both quantities reach a plateau after some downstream distance. The constancy of S_u and G_u/R_λ suggests that a dynamical equilibrium is attained between the production and destruction of $\overline{\varepsilon}$ which explains the emergence SP solutions. However, as in the case of the centreline evolution of Re_λ (fig. (4)), the distance x/D before the plateau is reached increases as Re_D increases. Thus, it appears that the establishment of the dynamical equilibrium is also function of the jet Reynolds number; the higher Re_D is, the longer it takes for the turbulence decay to reach its equilibrium.

Since both S_u and R_λ are constant, G_u must also be

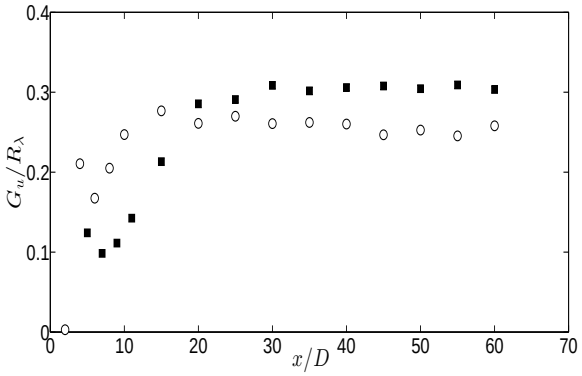


Figure 6. Centreline variation of G_u/R_λ. Symbols same as in fig. (5).

constant. While it may not be simple to show that G_u/R_λ is constant when SP is satisfied, the constancy of S_u can easily be shown as follows. S_u can be expressed as

$$S_u = lim_{r\to0}\frac{\overline{(\delta u)^3}}{\overline{(\delta u)^2}^{3/2}} \tag{9}$$

Since SP solutions for eq. (2) are sought in the form of

$$\overline{(\delta u)^2} = u^{*2} f(r/l) \tag{10}$$

and

$$\overline{(\delta u)^3} = u^{*3} h(r/l) \tag{11}$$

at all scales, where u^* is a scaling velocity and l a scaling length, then it is evident that S_u must be constant since the ratio $\frac{h(r/l)}{f(r/l)^{3/2}}$ is constant at all scales, which includes the scales when $r\to0$, in the SP region of the jet. Interestingly, this shows that SP solutions to single-point equations must also be compatible with SP solutions to two-point equations. Accordingly, one expects that a two-point SP analysis provides more information than a single-point SP analysis. Note though that carrying out a SP analysis to Eq. (3) can lead to the power-law $\overline{\varepsilon}\sim x^{-4}$. Indeed, applying a SP analysis to the mean momentum equation (*e.g.*Townsend (1956)) leads to $\overline{q^2}\sim\overline{u^2}\sim\overline{v^2}\sim x^{-2}$ and $U\sim x^{-1}$, which, when substituted into eq. (3), yields $\overline{\varepsilon}\sim x^{-4}$, as it should be.

Having established that R_λ, S_u and G_u are constant when the turbulence decays in a SP manner on the centreline of the round jet, we shift our attention to the relation (4). The relation has been analysed by Thiesset *et al.* (2014) in the context of the approach toward the asymptotic state at infinite Reynolds number. This approach is represented in Figure (7), which shows the expression $\frac{90}{7(2+R)R_\lambda}$ with $R = 2/3$ as function of R_λ; the measured values of the sum $S_u + 2G_u/R_\lambda$ for $Re_D = 2\times10^4$ and 8.9×10^4 are also reported on the figure. The experimental data appear to be in a relatively good agreement with the theoretical prediction, to within the uncertainty errors. It is evident though that beyond a value of $R_\lambda \geq 200$, the comparison between theory and measurement is difficult, since the values of $S_u + 2G_u/R_\lambda$ fall within the measurement uncertainty. The comparison should be better assessed at lower

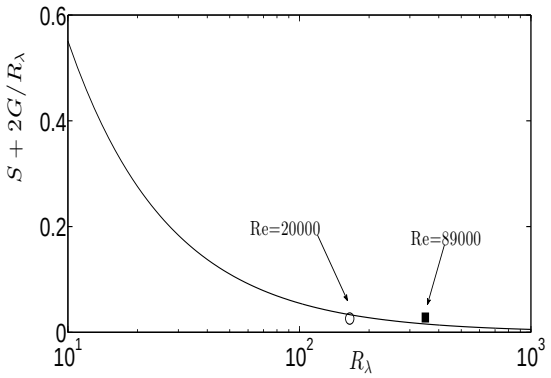


Figure 7. $S_u + 2G_u/R_\lambda$ as function of R_λ. Line: $\frac{90}{7(2+R)R_\lambda}$. Symbols: measurement, same as in fig. (5).

Reynolds numbers where $S_u + 2G_u/R_\lambda$ is relatively large and beyond the measurement uncertainty.

The predicted trend of $(S_u + 2G_u/R_\lambda)$ as $R_\lambda \to \infty$, which is consistent with the experimental data, shows that the balance between the production and destruction of $\overline{\varepsilon}$ must decrease with increasing Reynolds number. Eventually when $R_\lambda \to \infty$ the right side of (4) becomes zero, which corresponds to steady state solutions and one recovers the Kolmogorov hypothesis which states that at a very high Reynolds number the small-scale motions are in a steady state.

Eq. (4) shows that the large-scale anisotropy parameter R plays a role in the approach toward the steady state, although that role diminishes with an increasing R_λ. Accordingly, if one accepts that R is dependent on the initial contritions, one must then envisage that the approach $(S_u + 2G_u/R_\lambda) \to 0$ as $R_\lambda \to \infty$ to be also dependant of the initial conditions. It is then reasonable to expect, as Thiesset *et al.* (2014) argued, that the route toward the stationarity may not be universal. Further, since the various contributions from the large scales change in the transport equation for $\overline{(\delta u)^2}$ across the jet, the relation (4) varies too. Thus, one expects that the route to the steady state solutions also will vary from position to position across the width of a given jet. One can also argued that the route to stationarity will change from flow to flow. Thiesset *et al.* (2014) discussed the route the small scales follow in decaying grid turbulence, where if one assumes $\overline{\varepsilon} = A(x-x_o)^{n-1}$ $(n \leq -1)$, then the isotopic form corresponding to eq. (4) is given by (*e.g* Batchelor & Townsend (1947),

$$S_u + 2G_u/R_\lambda = \frac{90}{7(2+R)}\left(\frac{n-1}{n}\right)\frac{1}{R_\lambda}. \qquad (12)$$

Clearly, as R_λ increases, the sum $S_u + 2G_u/R_\lambda$ in grid turbulent follows a route different to that on the centreline of the turbulent round jet, which, as pointed out by Thiesset *et al.* (2014), casts doubts on the idea that S_u and G_u follow a universal evolution as $R_\lambda \to \infty$.

CONCLUSION

Hot wire measurements are carried out on the axis of a turbulent round jet to investigate the transport equation of the mean turbulent kinetic energy dissipation rate $\overline{\varepsilon}$ within the framework of the scale-by-scale (sbs) energy budget equation. The study completes and extends the analytical work of Thiesset *et al.* (2014).

It is confirmed that $\overline{\varepsilon} \sim A_\varepsilon(x-x_o)^{-4}$ as predicted by Thiesset *et al.* (2014) after applying a self-preservation (SP) analysis to the sbs equation on the centreline of the jet. Further, the measured values of A_ε agree relatively well with the prediction of Thiesset *et al.* (2014). Also, as required by SP, the Taylor microscale Reynols number R_λ is found to be constant along the centreline. However, it is observed that the distance x/D before R_λ becomes constant (*i.e.* that SP is attained) increases with the jet Reynolds number Re_D.

The isotropic form of the transport equation of $\overline{\varepsilon}$, as expressed by eq. (4), is analysed with the view to assess the behaviour of its individual terms during the decay. The measurements show that all individual terms of eq. (4) become independent of x/D when SP of attained. However, the distance x/D before this is achieved increases with the Reynolds number.

Finally, the measurements support the theoretical prediction of Thiesset *et al.* (2014) which shows that the balance between the production and destruction of $\overline{\varepsilon}$ decreases like C/R_λ^{-1}, where C is a constant. This shows that when $R_\lambda \to \infty$ the small scales approach stationarity. However, because the constant C is controlled by the large-scale anisotropy, the route toward stationary is likely to change from position to position across the jet width. Further, since the effects of large-scale anisotropy is felt differently from flow to flow, one expects that different routes to stationarity will be followed by different turbulent flows. This supports the argument put forward by Thiesset *et al.* (2014) that the manner by which the small scales approach stationarity as the Reynolds number increases is not universal and is flow dependent.

REFERENCES

Antonia, RA & Mi, J. 1993 Temperature dissipation in a turbulent round jet. *Journal of Fluid Mechanics* **250**, 531–551.

Antonia, RA, Satyaprakash, BR & Hussain, AKMF 1980 Measurements of dissipation rate and some other characteristics of turbulent plane and circular jets. *Physics of Fluids (1958-1988)* **23** (4), 695–700.

Batchelor, GK & Townsend, AA 1947 Decay of vorticity in isotropic turbulence. *Proceedings of the Royal Society of London. Series A. Mathematical and Physical Sciences* **190** (1023), 534–550.

Burattini, P, Antonia, RA & Danaila, L 2005*a* Similarity in the far field of a turbulent round jet. *Physics of Fluids (1994-present)* **17** (2), 025101.

Burattini, P., Antonia, R. A. & Danaila, L. 2005*b* Scale-by-scale energy budget on the axis of a turbulent round jet. *Journal of Turbulence* **6**.

Darisse, A., Lemay, J. & Benaissa, A. 2014 Extensive study of temperature dissipation measurements on the centreline of turbulent round jet based on the $\theta^2/2$ budget. *Exp. Fluids* **55:1623**, 1 – 15.

Ewing, D., Frohnapfel, B., George, W.K., Pedersen, J.M. & Westerweel, J. 2007 Two-point similarity in the round jet. *J. Fluid Mech.* **577**, 309 – 330.

Friehe, C. A., Van-Atta, C.W. & Gibson, C.H. 1971 Jet turbulence dissipation rate measurements and correlations. In *AGARD, Conference Proceedings*, , vol. 93.

George, W. K. 1989 *The self-preservation of turbulent flows and its relation ti initial conditions and coherent structures*. Hemisphere NY.

George, W. K. & Gibson, M. M. 1992 The self-preservation

of homogeneous shear flow turbulence. *Expts. Fluids* **13**, 229–238.

Kahalerras, H, Malecot, Y, Gagne, Y & Castaing, B 1998 Intermittency and reynolds number. *Physics of Fluids* **10** (4), 075101.

Mi, J, Xu, M & Zhou, T 2013 Reynolds number influence on statistical behaviors of turbulence in a circular free jet. *Physics of Fluids* **25** (7), 075101.

Panchapakesan, NR & Lumley, JL 1993 Turbulence measurements in axisymmetric jets of air and helium. part 1. air jet. *Journal of Fluid Mechanics* **246**, 197–223.

Taub, G.N., Lee, H., Balachandar, S. & Sherif, S.A. 2013 A direct numerical simulation study of higher order statistics in a turbulent round jet. *Physics of Fluids (1994-present)* **25** (11), 115102.

Thiesset, F, Antonia, RA & Djenidi, L 2014 Consequences of self-preservation on the axis of a turbulent round jet. *Journal of Fluid Mechanics* **748**, R2.

Townsend, A. A. 1956 *The Structure of turbulent shear flow, 1st ed.*. Cambridge University Press.

Wygnanski, I., Champagne, F. & Marasli, B. 1986 On the large-scale structures in two-dimensional, small-deficit, turbulent wakes. *J. Fluid Mech* **168**, 31–71.